Published in final edited form as:
Brain Res. 2008 May 23; 1211: 6–12. doi:10.1016/j.brainres.2008.03.014.

Fewer active motors per vesicle may explain slowed vesicle transport in chick motoneurons after three days in vitro

Jed C. Macosko[1], **Jason M. Newbern**[2], **Jean Rockford**[1], **Ernest N. Chisena**[1], **Charlotte M. Brown**[1], **George M. Holzwarth**[1], and **Carol E. Milligan**[2]

1*Department of Physics, Wake Forest University Winston-Salem, NC 27109*

2*Department of Neurobiology and Anatomy, Wake Forest University School of Medicine*

Abstract

Vesicle transport in cultured chick motoneurons was studied over a period of 3 days using motion enhanced differential interference contrast (MEDIC) microscopy, an improved version of video-enhanced DIC. After 3 days in vitro (DIV), the average vesicle velocity was about 30% less than after 1 DIV. In observations at 1, 2 and 3 DIV, larger vesicles moved more slowly than small vesicles, and retrograde vesicles were larger than anterograde vesicles. The number of retrograde vesicles increased relative to anterograde vesicles after 3 DIV, but this fact alone could not explain the decrease in velocity, since the slowing of vesicle transport in maturing motoneurons was observed independently for both anterograde and retrograde vesicles. In order to better understand the slowing trend, the distance vs. time trajectories of individual vesicles were examined at a frame rate of 8.3/s. Qualitatively, these trajectories consisted of short (1–2 s) segments of constant velocity, and the changes in velocity between segments were abrupt (<0.2 s). The trajectories were therefore fit to a series of connected straight lines. Surprisingly, the slopes of theses lines, i.e. the vesicle velocities, were often found to be multiples of ~0.6 μm/s. The velocity histogram showed multiple peaks, which, when fit with Gaussians using a least squares minimization, yielded an average spacing of 0.57 μm/s (taken as the slope of a fit to peak position vs. peak number, $R^2 = 0.994$). We propose that the abrupt velocity changes occur when 1 or 2 motors suddenly begin or cease actively participating in vesicle transport. Under this hypothesis, the decrease in average vesicle velocity observed for maturing motoneurons is due to a decrease in the average number of active motors per vesicle.

Classification terms

Theme B (Cellular and Molecular Biology) Topics—“Cytoskeleton transport and membrane targeting” and “Staining, tracing, and imaging techniques”

Section

Cellular and Molecular Biology of Nervous Systems

Correspondence address: Jed C. Macosko, Ph.D., Department of Physics, Wake Forest University, Winston-Salem, NC 27109, (336) 758-7981, (336) 758-6142 (fax), macoskjc@wfu.edu, http://www.wfu.edu/~macoskjc.
Present address: J.M. Newbern, UNC Neuroscience Center, 105 Mason Farm Rd, CB7250, University of North Carolina School of Medicine, Chapel Hill, NC 27599

Keywords

Processive molecular motors; cooperative fast axonal transport; anterograde neuron traffic; retrograde vesicle velocity; video enhanced differential interference contrast microscopy (VE-DIC); in vitro neuronal aging

1. Introduction

Radioactive tracer studies show that fast transport of protein-containing lipid-enclosed vesicles occurs at average speeds ranging from 0.6 to 32 μm/s (reviewed in Dahlstrom 1971; Ochs 1972). It is now firmly established that molecular motors perform the task of moving such cargo along cytoskeletal filaments (Schliwa and Woehlke 2003). Much understanding about the mechanics of motor proteins, such as their velocity under various loads—i.e. their force-velocity curves—has been gained by in vitro work (Block 1998; Vale 2003) but some questions remain, such as, "Do multiple motors cooperate to regulate transport velocity?" In an effort to better understand molecular motor driven transport, we chose to examine vesicle velocities in motoneurons from the spinal cords of chicken embryos.

Primary cultures of spinal motoneurons from chicken embryos have been utilized as a model system for neuronal differentiation, outgrowth, and survival (Sato et al. 2002). Such motoneurons can extend axons over long distances (mm to cm), a feature that may contribute to their vulnerability to mutations in intracellular transport proteins. Indeed, abnormalities in motoneuron axonal transport has been implicated in a variety of neurodegenerative conditions (Gunawardena and Goldstein 2004). Thus, determining correlations between fast vesicle transport and motoneuron maturation could elucidate the underlying mechanisms of some diseases. In this study, motion enhanced differential interference contrast (MEDIC, Fig. 1) microscopy was used to examine the relationship between total time of maturation (in vitro), vesicle size, and the direction and velocity of fast vesicle transport in the neurites. The distribution of velocities exhibited by a single vesicle was found to support a hypothetical model of transport in which 1–6 motors pull loads together in order to overcome viscous drag. We suggest that the observed decrease in transport velocity as motoneurons mature for three days in vitro occurs because fewer motors are actively transporting each vesicle.

2. Results

Position Versus Time Graphs of Vesicle Motion Show Abrupt Changes in Velocity

Two methods were used to determine vesicle displacement as a function of time. In the first method ("automated"), displacement in each frame was determined by an automated cross-correlation algorithm. The second method ("manual") displacement was determined only between the first and last frame of a vesicle's trajectory. In displacement versus time trajectories determined by the automated method (Fig. 2), velocities typically remained constant over short time periods (1–2 s, i.e. 8–17 frames) but were observed to abruptly change within one frame. Because of this behavior, the trajectories were not smoothed. Instead each trajectory was fit by a series of connected straight-line segments (see Experimental Procedures). The slope of each segment is the velocity at that time; for the vesicle in Fig. 2, the velocities range from 0.40 μm/s to 2.4 μm/s. In this case, six line segments minimized the reduced mean-squared error, χ^2_{red} to 1.12 (Fig. 2). This low value of χ^2_{red} demonstrates that the line-segment model is a statistically acceptable method of fitting the data. The reason for these abrupt velocity changes is discussed below.

Changes in Average Vesicle Speed and Direction as a Function of Day in Vitro (DIV)

Table 1 shows the number of visually observable vesicles (diameter > 0.1 μm and tracked by the "manual" method [see Experimental Procedures]) moving in the anterograde and retrograde directions and the average speeds at which they travel. A total of 601 vesicles in 106 movies were analyzed. These movies were taken over a set of 28 motoneurons, which varied from 1 to 3 DIV. Interestingly, the observed vesicles tended to move only in one direction, with <5% of the vesicles reversing directions and with these reversals lasting <1 s before the original direction is resumed.

Between the first and second day in culture there was already a significant ($p<0.05$) drop in the proportion of anterograde vesicles. By day 3, there was an equally significant drop in velocity (though, as described below, this drop occurred at day 2 for the subset of higher-contrast vesicles that could also be tracked with the "automated" method). Over this time period, there is no change in motoneuron viability when the cells are supplied with trophic support (Milligan et al., 1994). Cells observed in these experiments exhibited extensive neurite outgrowth and phase bright cell bodies.

Histograms of average vesicle speed in the day 1 and day 3 data show these two trends (Fig. 3). In addition, they demonstrate that the average speeds are, for the most part, normally distributed around the averages. As will be shown below, this normal distribution is not observed in the histograms of the individual vesicle velocity segments (e.g. the line segments of Fig. 2).

Anterograde Vesicles Are Faster, While Retrograde Vesicles Are Larger

In Table I, the anterograde velocity is significantly higher than the average retrograde velocity, averaged over all three days (1.70 ± 0.05 vs. 1.31 ± 0.04 μm/s, n=601). However, this trend may be related to another factor: retrograde vesicles tend to be larger. The overlaid histograms in Fig. 4 reveal the lopsided nature of vesicle transport in chick motoneurons. Over 75% of large vesicles, defined as those over 0.8 μm in apparent diameter, travel in the retrograde direction. On the other hand 55% of small vesicles, defined as those with an apparent diameter less than 0.6 μm, travel in the anterograde direction. The relationship between vesicle radius and speed, combined with the observation that retrograde vesicles are larger and become more prevalent with time, could explain the decrease in average velocity. But investigation of the *instantaneous* velocity using automated subpixel tracking revealed a different possible explanation.

Instantaneous Velocity Distribution Has Multiple, Evenly Spaced Peaks

As explained above and in the Experimental Procedures, it is possible to use the automated tracking method to determine the instantaneous subpixel position of an individual vesicle as a function of time. Interestingly, the velocities determined from these position versus time graphs (e.g. Fig. 2) were often roughly an integer multiple of 0.6 μm/s. For example, the first line segment fit in Fig. 2 has a slope of 2.4 μm/s (i.e. 0.6×4) and the last line segment has a slope of 1.8 μm/s (i.e. 0.6×3).. To better quantify this observation, we pooled the velocities from several such graphs (30 retrograde trajectories, 2075 data points from 1 DIV [32%], 2 DIV [59%], and 3 DIV [9%]) and created a velocity histogram (Fig. 5)

Remarkably, a pattern of evenly spaced peaks emerges from this type of histogram (Fig. 5). To determine the position of the peaks, we used a least squares minimization in Excel to perform a multi-Gaussian fit, constraining the center of first Gaussian to 0 μm/s. The largest Gaussian, encompassing 760 data points from 95 segments (37% of the observed velocities), is centered at 0.6 μm/s. Subsequent Gaussians decrease in size and are centered at 1.3, 1.8, 2.2, 3.1, and 3.7 μm/s. Based on a linear fit to a plot of Gaussian position vs. peak index, the average spacing

between the peaks is 0.59 μm/s (Fig. 5, inset). As will be discussed shortly, we suggest that these regularly spaced peaks are due to 0, 1, 2, etc. motor proteins actively transporting each vesicle during each time segment.

To determine what effect time in vitro had on peak spacing, we separated the instantaneous velocity by day. Unfortunately, the automated, subpixel tracking used to collect instantaneous velocities (see Experimental Procedures) was less successful with movies collected at 3 DIV, so we pooled the data from day 3 (9% of the total data) with day 2 (59% of the data) and used them in comparisons with vesicles from 1 DIV. For these two data sets, the average spacing between peaks was found to agree within <3% (0.61 and 0.59 μm/s, respectively, R^2=0.999 and 0.994, respectively). The effect of time in vitro on the averages of these instantaneous velocities was more pronounced and was consistent with the effect of time on the average velocities reported in Table 1 and Fig. 3: vesicles moved 17% slower at 2 and 3 DIV relative to 1 DIV (1.02±0.02 vs. 1.23±0.05 μm/s). Approximately $1/5^{th}$ of this drop can be attributed to an increased prevalence of paused segments (~0 μm/s, i.e. roughly zero active motors per vesicle) at 2 and 3 DIV relative to 1 DIV, since when segments with speeds <0.2 μm/s are removed from all the data, the net slow down from 1 to 2 and 3 DIV is only 13.3%.

Despite the qualitative similarity between the averages of the vesicles' *instantaneous* velocities, as determined by the automated method, and the averages of the vesicles' *average* velocities, as determined by the manual method (Table 1 and Fig. 3), these two averages differ quantitatively in two important respects: the decrease in average instantaneous velocity occurs earlier, by 2 DIV instead of by 3 DIV, and the average instantaneous speeds are lower. The reason for the lower speeds—e.g. 1.23 μm/s (automated, DIV 1) vs. 1.50 μm/s (manual, DIV 1)—is that the automated tracking program can not track the smallest and fastest vesicles, whereas manual tracking can. This reason may also explain the different onset of vesicle slow-down. For example, the smallest and fastest vesicles may slow down later than larger and slower vesicles thereby delaying the slow-down onset for Table 1 (manual) but not for the instantaneous velocity averages (automated). Given that the instantaneous velocity data was sparse at 3 DIV (only 9% of the occurrences), this earlier onset of slow-down was what allowed a comparison of peak spacing in a fast and in a slow data set, i.e. in 1 DIV and in 2+3 DIV, and showed that time in vitro affects the average velocity but not the peak spacing. While the difference between the effect of day in vitro on the peak spacing and average velocity (at first glance) appears mundane, it plays an important role in the physical mechanism that causes the observed slowing in transport velocity.

3. Discussion

Vesicle velocities correlate with neuron maturation

We have shown that the average speed of vesicle transport decreases as motoneurons mature in vitro. However, since, by Stokes' law, larger vesicles experience higher drag forces, it is important to understand the slowing trend vis-à-vis two other related observations. First, the proportion of transport in the retrograde direction increases with time in vitro (Fig. 3 and Table I). Second, since retrograde transport is slower than anterograde transport (Table 1), an increasing proportion of vesicles moving in the retrograde direction would cause a decrease in average speed. These two observations, then, could explain the decreasing average velocity observed for increasing day in vitro.

Although the preceding argument gives what is a rather prosaic accounting for the observed changes in velocity, Fig. 3 suggests that this may not be the whole story. In Fig. 3 we see a decrease in speed as a function of day in culture for *both* anterograde and retrograde transport. Consequently, although Fig. 4 shows a retrograde bias for larger (and therefore slower) vesicles, the increased proportion of retrograde transport in older motoneurons cannot fully

explain this observed slow-down, since anterograde and retrograde vesicles independently display this trend. Instead, there must be an alternative reason for the net decrease in average vesicle velocity as cells mature.

Four possible reasons for the slow-down immediately come to mind. First, the number of obstacles in the vesicle's path could be increasing. This could include contact with the plasma membrane at the cargo's destination point or at a zone of nonhomogenity and would create a higher drag force on the vesicles and cause the motors to operate more slowly. Second, the average size of both anterograde and retrograde vesicles could be increasing, which would have the same effect as higher viscosity. Third, the slow-down could be related to a decrease in the efficiency of each motor. Fourth, the distribution of the number of motors actively transporting each vesicle could be changing. For example, if n_1, n_2, and n_3 are the numbers of anterograde or retrograde vesicles traveling at v_1, v_2, and v_3, then the average transport velocity, $\overline{v}$, is a weighted average:

$$\overline{v}=\frac{v_1n_1+v_2n_2+v_3n_3}{n_1+n_2+n_3} \qquad \text{eq. 1}$$

Note that the peaks v_1, v_2, and v_3 in the velocity histogram do not change with day in vitro. However, if n_3 decreases relative to n_1 or n_3, the overall transport velocity, $\overline{v}$, would decrease. Furthermore, this drop in speed could occur without changes in vesicle size or cellular viscosity.

Our proposal, that the distribution of motors explains the observed slowing, hinges on the idea that two or more motors can distribute the drag force produced by a vesicle. Evidence for this idea was first provided by the motility assays of Hunt, Gittes and Howard in 1994 (Hunt et al. 1994). They showed that, when propelling a microtubule load against a viscous drag, the more kinesins that were attached to the load the faster the load would be moved, and they suggested that two motors would double the speed relative to single motor velocities. Since 1994, some studies in living cells have suggested a similar doubling (or tripling, etc.) of transported cargo velocities. For example, in 2004, Hill et al. (Hill et al. 2004) showed a velocity histogram of evenly spaced peaks for vesicles transported in PC12 cells similar to the histogram for chick motoneurons (Fig. 5). Peroxisomes transported in Drosophila cells and melanosomes transported in Xenopus melanophores also show a regularly spaced pattern of velocities (Kural et al. 2005; Levi et al. 2006). Furthermore, human NT2 cells reveal an identical pattern of peaks in the velocity histogram for vesicles that are transported within the cytosol rather than within neurites (Shtridelman et al. in preparation). Interestingly, when older data is reexamined, from the chick and rat neuron studies of Breuer et al. in 1975 to the more recent studies of C. elegans in 2004, the same regularly spaced pattern of peaks is seen (Breuer et al. 1975; Zahn et al. 2004). Some of these studies attributed the pattern to "two or more *different* molecular motors" [emphasis added] (Zahn et al. 2004), but perhaps a more parsimonious explanation is that multiple motors of the *same* type account for the successively higher velocity peaks. For example the pattern in velocity histograms of Drosophila peroxisomes, which extends out to 12 peaks, was attributed to "multiple kinesins or multiple dyneins" (Kural et al. 2005). (Kinesins and dyneins are known to transport organelles anterogradely and retrogradely, respectively, in axons). (Chevalier-Larsen and Holzbaur 2006; Morris and Hollenbeck 1993).

Returning to the three possible explanations for vesicle transport slow-down (viscosity, size, or number of active motors), our data support a slow-down model based on the number of motors. This is due to the fact that the peak spacing in Fig. 5 does not appreciably change (<3%) with day in vitro even as the overall velocity slows by 17%. Therefore, in accordance with the predicted effects on peak spacing of increasing size, increasing viscosity, and decreasing numbers of motors (eq. 1), it is more likely that the observed slow-down is due to a decrease in the number of motors actively pulling each vesicle.

Many questions about vesicle transport still remain. Can processive motors coordinate their steps so as to share their common load? What is the exact mechanism of the abrupt velocity changes seen in Fig. 2? How are vesicle transport speed and direction regulated? Will a global mechanism (e.g. phosphorylation, small GTPases, calcium flux, etc. (Muresan 2000)]) be discovered that controls the number of motors per vesicle irrespective of the motor type, or is there a separate regulatory pathway for each kind of motor protein? These questions await further study. In the meantime, we conclude that analyzing vesicle transport as a function of day in vitro reveals new aspects of neuronal growth, which, in this present work, has uncovered interesting correlations between neuronal maturation and the average and instantaneous vesicle transport velocities.

4. Experimental Procedures

Cell Preparation [For additional details, see (Milligan 1994)]

Spinal cords from embryonic day-5.5 chicks were dissected in cold phosphate-buffered saline and incubated in 0.05% trypsin at 37°C for 20 minutes. The tissue was triturated and the dissociated cell suspension was layered onto a 5% (v/v) iodixonal cushion (Optiprep, Sigma) and centrifuged at 900g for 15 minutes. Motoneurons were collected from the interface, and cellular debris was removed by further centrifugation on a 4% bovine serum albumin cushion. 1×10^5 of the resulting isolated motoneuron cells were plated on 50-mm glass-bottom tissue culture dishes coated with 10 μg/ml laminin and 2 μg/ml poly-ornithine. Between 70 and 90% of cells obtained by this procedure are motoneurons, as determined by immunostaining for the motoneuron-specific homeodomain transcription factor islet-1 (Milligan 1994). Cells were cultured in Leibovitz's L15 media supplemented with sodium bicarbonate (625 μg/ml), glucose (20 mM), progesterone (2×10^{-8} M), sodium selenite (3×10^{-8} M), conalbumin (0.1 mg/ml), putresine (10^{-4} M), insulin (5 mg/ml), and penicillin-streptomycin. Muscle extract (20 μg/ml) was added to provide trophic support for the motoneurons (Oppenheim 1988). Cultures were incubated in a 5.0% CO_2 atmosphere at 37°C with saturated humidity for 1, 2 or 3 days in vitro (DIV).

Microscopy and Image Acquisition

Images were generated by a Nikon E600 FN microscope equipped with a 60X water immersion objective (NA 1.0), an NA 0.9 condenser, DIC optics, a Hamamatsu ORCA ER camera (8.3 fps), and a standard 100-watt tungsten light source filtered to transmit 550 nm light. The contrast of moving vesicles was increased by more than a factor of 10 by applying real-time MEDIC ("motion-enhanced DIC") image processing to the raw, 12-bit DIC images. MEDIC is an extension of video-enhanced DIC (VE-DIC) (Allen 1985; Allen and Allen 1983; Allen et al. 1981), which replaces manual acquisition of a background image with a continuously updated, automatically generated, rolling average background image. MEDIC is described in more detail elsewhere (Hill et al. 2004; Hill, Macosko and Holzwarth, in preparation). Using the MEDIC technique 0.1 μm diameter polystyrene beads moving 1 μm/s are at the limit of detectability, thus likely candidates for the vesicular organelles that we observe in this paper are mitochondria (Friberg et al. 1998), lysosomes (Bednarski et al. 1997), peroxisomes (Moreno et al. 1997), and phagosomes (Martin et al. 1999)—all of which are larger than 0.1 μm in neuronal cells.

The DIC phase offset (deSenarmont polarizer angle) was set as described previously (Holzwarth 2000), in order to maximize the signal-to-noise ratio. Source intensity was adjusted to fill the intensity range of the 12-bit CCD camera. Fig. 1 shows an example of a chick motoneuron imaged with normal DIC and with MEDIC.

A stage containing resistive heating strips, built in-house, was used to keep the temperature at 37°C. Cells remained free of significant bacterial contamination for >3 hours while imaging, and all data in this study was collected during the first 2 hours. Background subtracted images were displayed on an Image Systems M17L grayscale monitor, and up to 400 frames (512 × 512 pixel^2, which at 9.36 pixels/μm is 55 × 55 μm^2) were saved to the hard drive at one time. Some example movies can be viewed in the Supplemental Information (movie M1–movie M3).

Velocity Analysis

Vesicle positions were measured by an automated pattern matching technique utilizing normalized cross correlation functions, which provided sub-pixel localization of larger vesicles (>0.4 μm diameter, Hill et al. 2004; Hill, Macosko and Holzwarth, in preparation). For vesicles that were too faint or fast-moving for accurate subpixel tracking, a manual method of subtracting the initial and final position of the vesicles was used to obtain their average velocities. Even with this manual method, the smallest vesicles (<0.1 μm diameter) were probably not observed, since 0.1 μm polystyrene beads that were moved by a piezoelectric stage and imaged with MEDIC were only barely visible at the deSenarmont polarizer angle used for these chick motoneuron studies (Shtridelman et al. in preparation).

To analyze the velocity patterns for each vesicle, the position versus time trajectories were fitted with connected line segments. The χ^2_{red} value (the reduced mean-squared error) was calculated for each optimized line-segment model (York 1966). The optimal number of segments was determined by finding the lowest value of χ^2_{red}. Vesicle velocities corresponded to the slopes of the fitted line segments. The reason for fitting vesicle trajectories with line segments (instead of smoothing the data) is explained in the Results section.

Supplementary Material

Refer to Web version on PubMed Central for supplementary material.

Acknowledgements

We thank Anna Taylor for help with preparing chick motoneurons and Keith Bonin for helpful discussions. We gratefully acknowledge Todd Fallesen for input at various stages. This work was supported by a start-up grant by Wake Forest University to JCM and by an NIH grant (NS036081) to CEM.

References

Allen RD. New observations on cell architecture and dynamics by video-enhanced contrast optical microscopy. Annu Rev Biophys Biophys Chem 1985;14:265–290. [PubMed: 3890883]

Allen RD, Allen NS. Video-enhanced microscopy with a computer frame memory. J Microsc 1983;129 (Pt 1):3–17. [PubMed: 6827591]

Allen RD, Allen NS, Travis JL. Video-Enhanced Contrast, Differential Interference Contrast Microscopy. Cell Motility 1981;1:291–302. [PubMed: 7348605]

Bednarski E, Ribak CE, Lynch G. Suppression of cathepsins B and L causes a proliferation of lysosomes and the formation of meganeurites in hippocampus. J Neurosci 1997;17(11):4006–4021. [PubMed: 9151717]

Block SM. Kinesin: what gives? Cell 1998;93(1):5–8. [PubMed: 9546384]

Breuer AC, Christian CN, Henkart M, Nelson PG. Computer analysis of organelle translocation in primary neuronal cultures and continuous cell lines. J Cell Biol 1975;65(3):562–576. [PubMed: 48515]

Chevalier-Larsen E, Holzbaur EL. Axonal transport and neurodegenerative disease. Biochim Biophys Acta 2006;1762(11–12):1094–1108. [PubMed: 16730956]

Dahlstrom A. Axoplasmic transport (with particular respect to adrenergic neurons). Philos Trans R Soc Lond B Biol Sci 1971;261(839):325–358. [PubMed: 4111802]

Friberg H, Ferrand-Drake M, Bengtsson F, Halestrap AP, Wieloch T. Cyclosporin A, but not FK 506, protects mitochondria and neurons against hypoglycemic damage and implicates the mitochondrial permeability transition in cell death. J Neurosci 1998;18(14):5151–5159. [PubMed: 9651198]

Gunawardena S, Goldstein LS. Cargo-carrying motor vehicles on the neuronal highway: transport pathways and neurodegenerative disease. J Neurobiol 2004;58(2):258–271. [PubMed: 14704957]

Hill DB, Plaza MJ, Bonin K, Holzwarth G. Fast vesicle transport in PC12 neurites: velocities and forces. Eur Biophys J 2004;33(7):623–632. [PubMed: 15071760]

Holzwarth G, Hill D, McLaughlin E. Polarization-Modulated Differential-Interference Contrast Microscopy with a Variable Retarder. Applied Optics 2000;39(34):6288–6294. [PubMed: 18354637]

Hunt AJ, Gittes F, Howard J. The force exerted by a single kinesin molecule against a viscous load. Biophys J 1994;67(2):766–781. [PubMed: 7948690]

Kural C, Kim H, Syed S, Goshima G, Gelfand VI, Selvin PR. Kinesin and Dynein Move a Peroxisome in Vivo: A tug-of-war or Coordinated Movement? Science 2005;308:1469–1472. [PubMed: 15817813]

Levi V, Serpinskaya AS, Gratton E, Gelfand V. Organelle transport along microtubules in Xenopus melanophores: evidence for cooperation between multiple motors. Biophys J 2006;90(1):318–327. [PubMed: 16214870]

Martin EJ, Kim M, Velier J, Sapp E, Lee HS, Laforet G, Won L, Chase K, Bhide PG, Heller A, et al. Analysis of Huntingtin-associated protein 1 in mouse brain and immortalized striatal neurons. J Comp Neurol 1999;403(4):421–430. [PubMed: 9888310]

Milligan C. Motoneurons deprived of trophic support in vitro require new gene expression to undergo programmed cell death. J. Neurobiol 1994;25(8):1005–1016. [PubMed: 7964701]

Moreno S, Nardacci R, Ceru MP. Regional and ultrastructural immunolocalization of copper-zinc superoxide dismutase in rat central nervous system. J Histochem Cytochem 1997;45(12):1611–1622. [PubMed: 9389764]

Morris RL, Hollenbeck PJ. The regulation of bidirectional mitochondrial transport is coordinated with axonal outgrowth. J Cell Sci 1993;104(Pt 3):917–927. [PubMed: 8314882]

Muresan V. One axon, many kinesins: What's the logic? J Neurocytol 2000;29(11–12):799–818. [PubMed: 11466472]

Ochs S. Fast transport of materials in mammalian nerve fibers. Science 1972;176(32):252–260. [PubMed: 5019778]

Oppenheim R. Reduction of naturally occuring motoneuron death in vivo by target derived neurotrophic factor. Science 1988;240:919–922. [PubMed: 3363373]

Sato N, Sakuma C, Kato H, Milligan CE, Oppenheim RW, Yaginuma H. Bcl-2 rescues motoneurons from early cell death in the cervical spinal cord of the chicken embryo. J Neurobiol 2002;53(3):381–390. [PubMed: 12382265]

Schliwa M, Woehlke G. Molecular motors. Nature 2003;422(6933):759–765. [PubMed: 12700770]

Vale RD. The Molecular Motor Toolbox for Intracelllular Transport. Cell 2003;112:467–480. [PubMed: 12600311]

York D. Least squares fitting of a straight line. Canad. J. of Phys 1966;44:1079–1086.

Zahn TR, Angleson JK, MacMorris MA, Domke E, Hutton JF, Schwartz C, Hutton JC. Dense core vesicle dynamics in Caenorhabditis elegans neurons and the role of kinesin UNC-104. Traffic 2004;5(7):544–559. [PubMed: 15180830]

Abbreviations

DIV, day in vitro; NA, numerical aperture; fps, frames per second; MEDIC, motion enhanced DIC; DIC, differential interference contrast.

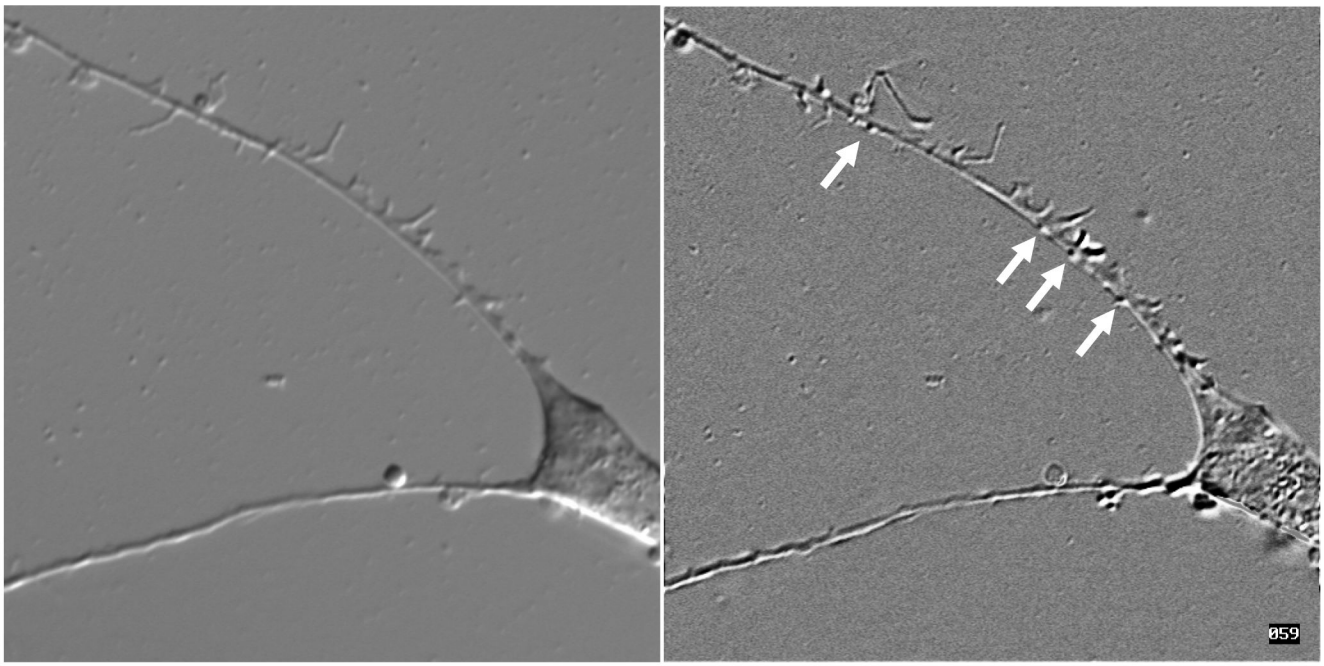

Fig. 1. DIC vs. MEDIC

In a traditional DIC image (left) the cell body and two processes are evident—but not the transported vesicles inside the two processes. In a MEDIC, or motion enhanced DIC, image of the same cell (right) moving vesicles are clearly seen (white arrows, see also Supplemental Information, Movie M1–Movie M3). A conspicuous difference in the number of filopodia on processes originating from the same cell, as is seen here, is typically observed in these chick motoneurons.

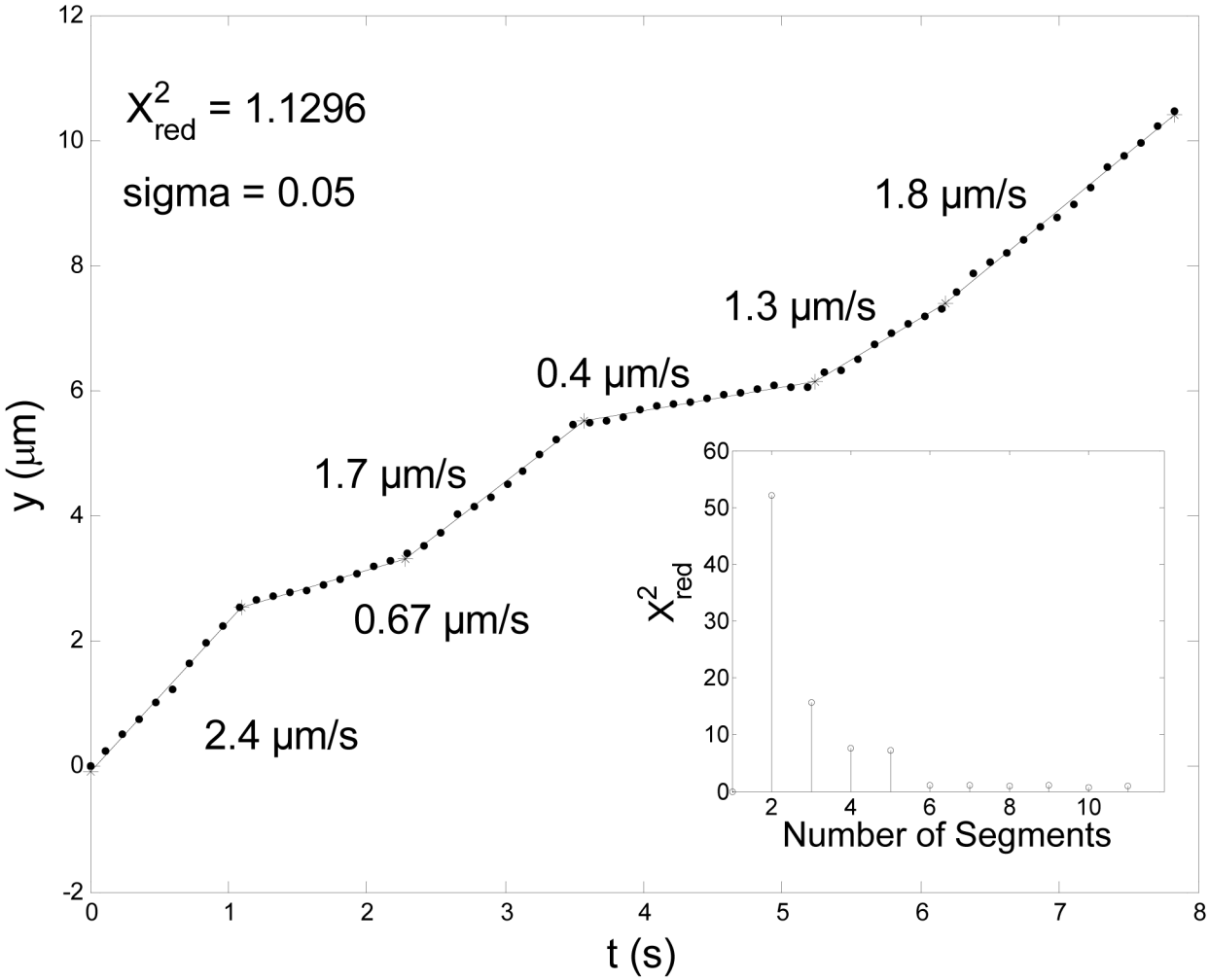

Fig. 2. Distance vs. time of a retrograde vesicle

Vesicle tracking data displays abrupt changes in velocity for most vesicles, including this one that traveled in the retrograde direction for 7.8 s (1.3 μm/s average speed). **Inset:** The values of χ^2_{red} for fitting 2 to 11 straight-line segments indicate that 6 segments are optimal. Line segments are fit to the data by a least squares optimization (MatLab Optimization Toolbox).

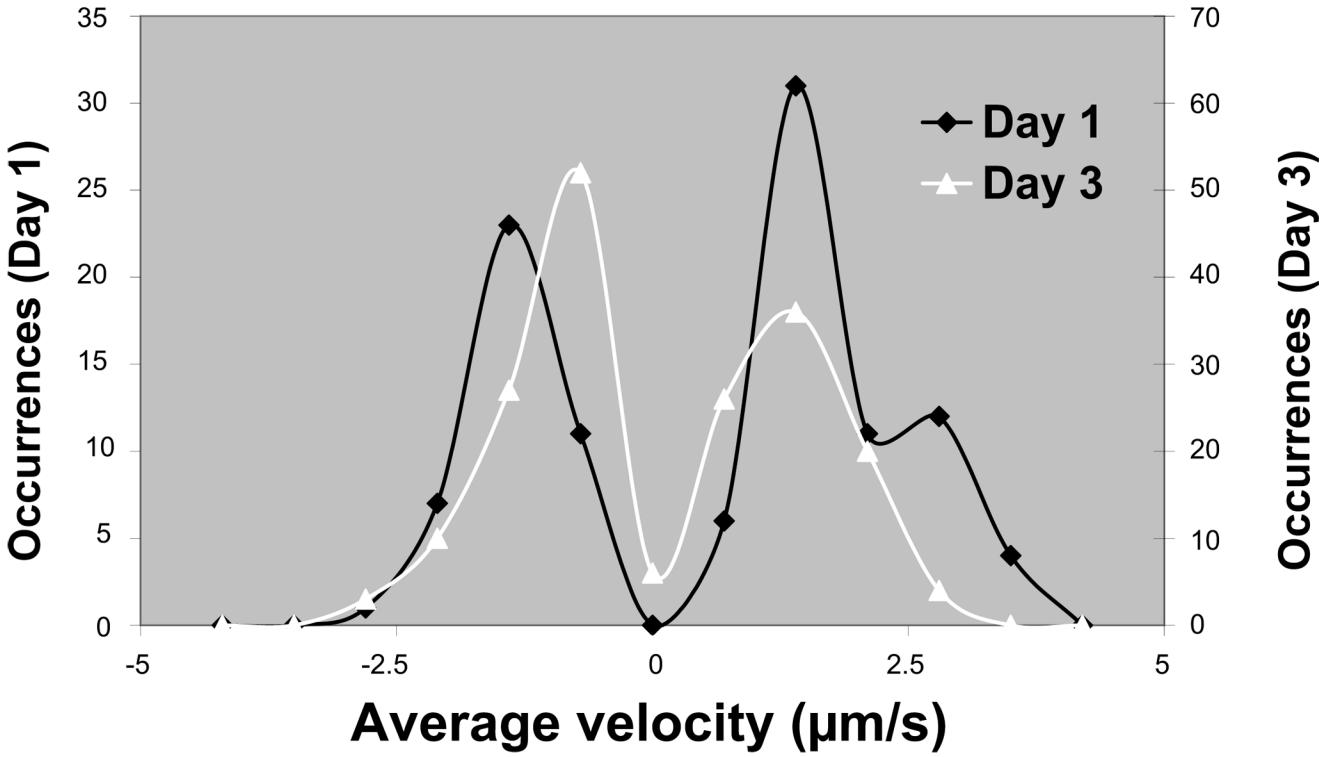

Fig. 3. Histograms of average velocities of individual vesicles at 1 or 3 days in vitro

Each occurrence is the average velocity of one vesicle (N=290) as determined by the manual method. The average speeds in either direction (anterograde velocities are indicated by positive values and retrograde by negative values) decrease as chick motoneurons are cultured for 3 days. A shift toward more retrograde transport is apparent in day 3 relative to day 1 (see also Table 1).

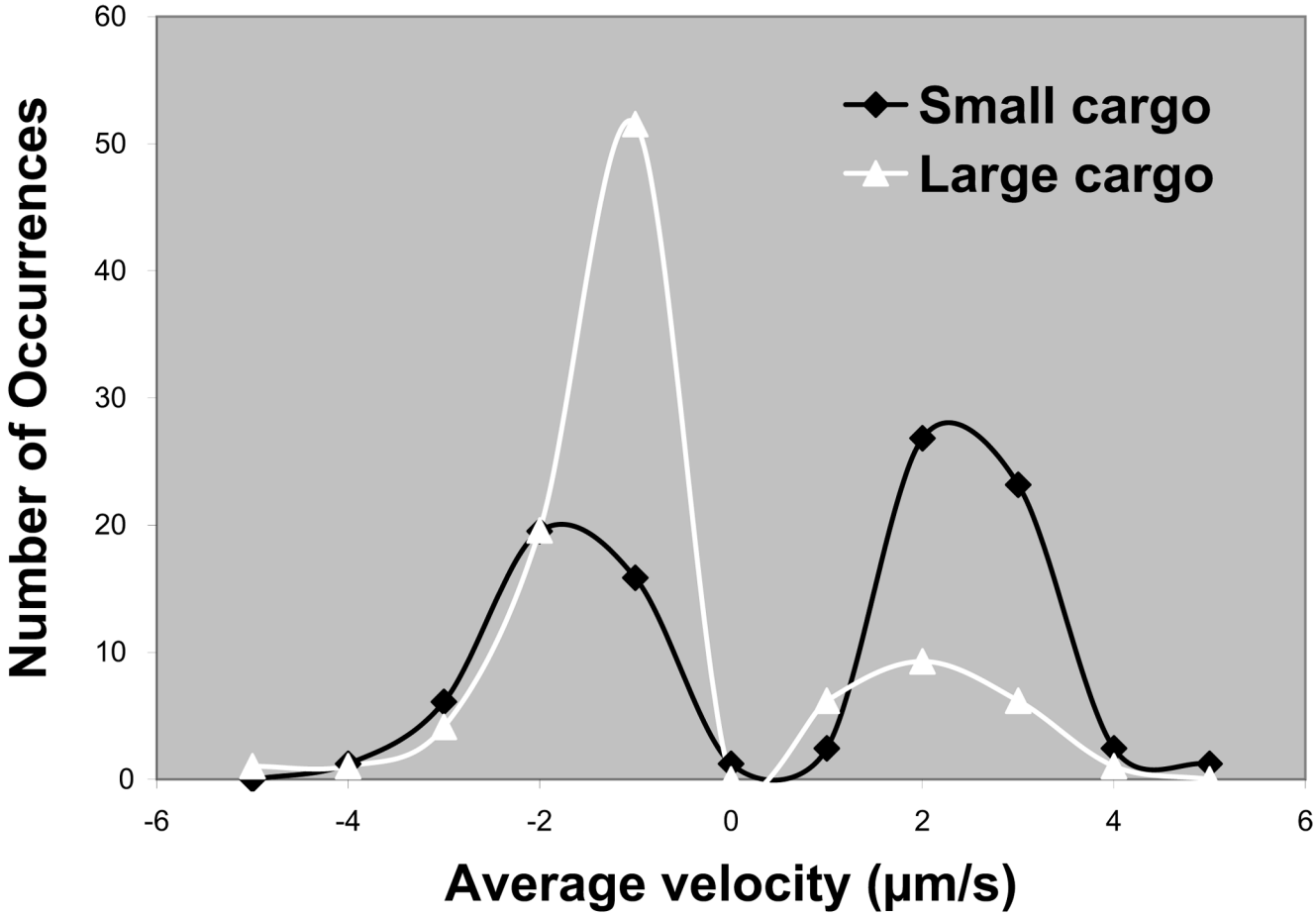

Fig. 4. Histograms of average velocities for large and small vesicles

Each occurrence corresponds to the average velocity of one vesicle (N=179, manual method). Large vesicles (>0.8 μm diameter) move predominantly in the retrograde direction and move slower than small vesicles (<0.6 μm diameter). The mean velocities for the four populations shown in this histogram are: small anterograde = 2.5 μm/s; large anterograde = 2.0 μm/s; small retrograde = 1.8 μm/s; and large retrograde = 1.4 μm/s. The prevalence of retrograde transport is >4-fold higher for large vesicles than for small (large = 3.4-fold more retrograde than anterograde, small = 1.3 fold less retrograde than anterograde).

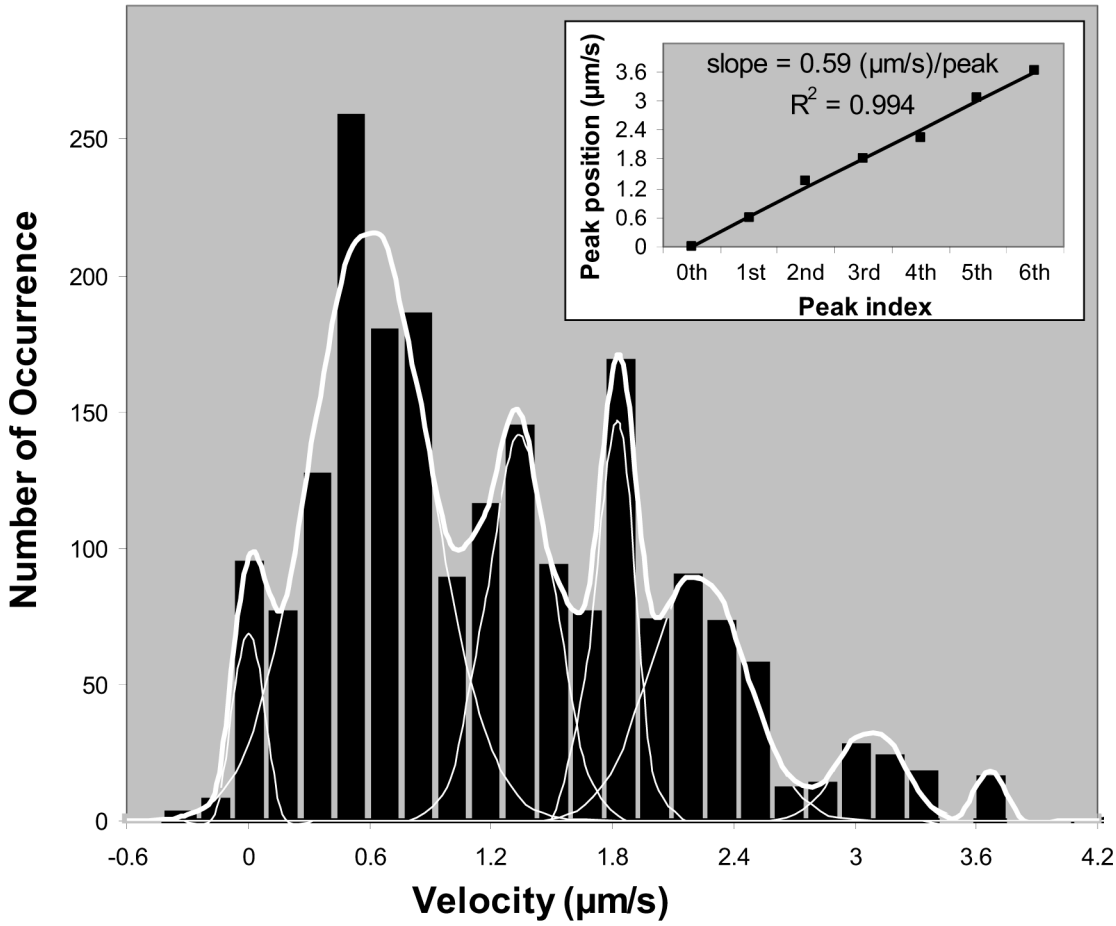

Fig. 5. Histogram of instantaneous retrograde velocities of individual vesicles

(frame rate = 8.3/s). Each occurrence corresponds to the slope of the best-fit line segment at each frame (N=2075) for vesicle trajectories on DIV 1, 2, and 3 obtained by the automated method (see Fig. 2). The histogram is binned at 1/6 µm/s intervals and fit (thick white curve) with 7 Gaussians (thin white curves) and one constraint (the first peak starts at 0 µm/s). The χ^2_{red} for this fit was 3.4. **Inset:** A graph of the peak positions vs. peak index for the multi-Gaussian fit reveals a regular 0.59 µm/s peak spacing (R^2=0.994).

Table 1

Vesicle direction and speed for motoneurons cultured for 1, 2, and 3 days.

	Occurrences		Speed† (μm/s±σ_m)	
	n_{antero}/n_{total}	%	retro	antero
day 1	73/131	56	1.5±0.08	1.8±0.09
day 2	116/258	45	1.5±0.06	1.9±0.08
day 3	99/212	47	1.0±0.05	1.3±0.06
all days	288/601	48	1.3±0.04	1.7±0.05
Δ(day1→3)	--	−16*	−33%±7%	−28%±6%

† Speed is the average of the individual vesicle velocities as determined by the manual method (vesicle displacement between first and last frame divided by elapsed time).

* The change in percent anterograde vesicles from day 1 to day 3 is calculated using the formula: $\frac{\%\text{ on day 3}}{\%\text{ on day 1}} - 1$